J. Chem. Sci. Vol. 127, No. 3, March 2015, pp. 575–581.
DOI 10.1007/s12039-014-0764-z

Atomistic understanding of hydrogen loading phenomenon into palladium cathode: A simple nanocluster approach and electrochemical evidence

MOHSEN LASHGARI[a,b,*] and DAVOOD MATLOUBI[a]

[a]Department of Chemistry, Institute for Advanced Studies in Basic Sciences (IASBS), Zanjan 45137-66731, Iran

[b]Centre for Climate Change and Global Warming: Hydrogen and Fuel Cell Laboratory, Zanjan 45137-66731, Iran

e-mail: Lashgari@iasbs.ac.ir

MS received 1 December 2013; revised 19 June 2014; accepted 9 July 2014

Abstract. The inherent potency of palladium to sorb hydrogen atoms was examined empirically and theoretically through various electrochemical methods and high-level quantum chemical calculations (HSE06) based on cluster model (CM) and density functional theory (DFT). The CM-DFT approach using QZVP/cc-PV6Z basis sets revealed a strong attraction between Pd nanoclusters and H atoms that generates some charged entities. This atomistically justifies why the electrochemical impedance of the system becomes less by the loading phenomenon. It is concluded that hydrogen atoms enter the palladium subsurface through hollow and bridge sites by diffusing as proton-like species and get loaded predominantly in the octahedral voids.

Keywords. Palladium electrode; H-loading/unloading; Pd nanoclusters; Pd/H interaction; electrochemical impedance spectroscopy.

1. Introduction

Hydrogen is the simplest, lightest and the most abundant element discovered in the universe. It is utilized continuously as a fuel of celestial power-generating nuclear-reactors in the sun and other stars.[1] The solar energy shining upon the earth every day can be transformed to electricity using a photon-to-electron convertor or stored chemically as hydrogen fuel in a photo-electrolyzing system.[2] This chemical energy can be released whenever required, effectively using a *cold combustion reactor*, so-called *fuel cell*.[3] Besides this method of releasing energy, there are also some controversial reports on excess-heat generation through nuclear reactions with elemental transmutation as the result of Pd/H interaction under ambient conditions, referred popularly as *cold fusion*.[4,5]

Concerning hydrogen storage and energy-related materials, it is worthy to note that palladium metal has a well-known potency to absorb hydrogen atoms.[6] The metal is also used widely in different industries, including pollutant controlling systems, hydrogen sensors, catalysts, etc.[7] Therefore, its interactional studies will be important from technological as well as scientific view points. In the present work, we have focused on this issue (Pd/H interaction[8]) from atomistic perspective. Here, the loading of hydrogen atoms is simply achieved through proton reduction process in a palladium electrode.[9,10] The experimental investigations were carried out through various electrochemical methods[11] and the H-unloading process[12] was also accomplished via atom oxidation (reconversion to proton) by applying a constant anodic voltage. For a better understanding of the phenomenon, the empirical observations are compared with those of Pt electrode. In the theoretical part, we adopt a sophisticated and simplified strategy; namely, the Pd/H interactions are considered locally and the calculations are restricted to particular zones of the system in the vicinity of H atom. Therefore, the interactions becomes crutinized through a straightforward route which utilizes high level quantum chemical calculations by means of molecular orbital theory and cluster model.[13,14] This strategy is totally different from that of periodic or slab approach that uses plane waves, rather than local basis sets. The aim of this complementary (theoretical) study is to arrive at some qualitative concluding remarks to rationalize the empirical evidence of H-loading phenomenon into palladium lattice.

*For correspondence

2. Experimental

2.1 *Electrochemical tests and setup*

Water electrolysis, cyclic voltammetry (CV), chronoamperometry (CA) and electrochemical impedance spectroscopy (EIS; the impedance of system ($Z = Z_{re} - jZ_{im}$; $j = \sqrt{-1}$) measured in a frequency range of applied AC signal[3,15]), were all carried out in a 3-electrode home-made 12 cm^3 cell, in which the working electrode was fixed in the bottom and the reference (SCE) and counter (Pt foil, 2 cm^2) were both hanged on the top of the cell. The working electrode was a Pd wire (SIGMA-ALDRICH®; diameter: 0.5 mm, assay: 99.9%), fixed in a glassy tube with a rubber cork. The tube then filled partially with epoxy resin. The palladium wire exposed to the electrolyte had 1.5 cm length. The electrolyte was 0.1 M NaOH solution prepared from triply distilled water. In each experiment, a fresh solution was applied. The electrochemical experiments were carried out through a Zahner/Zennium Potentio/Galvanostat Impedance workstation operating with the Thales Z1.15 software. The scan rate and frequency range were set at 100 mVs^{-1}[16] and 100 kHz to 10 mHz, respectively. The impedance spectra were analyzed using an EC-Lab® software (V10.22).

Gas volumetric measurement of hydrogen bubbles was performed using an inverted burette filled by the electrolyte, hung over the cathode. All experiments were triplicated and the mean value was reported as final datum.

2.2 *Cluster approach and computational strategy*

In cluster approach, the metal-species interactions are considered locally;[13,17] so, the interactions are limited to the portion of metal (substrate atoms) which is in the vicinity of sorbed-species. The system is treated as a supermolecule and its electronic structure is often determined through DFT quantum chemical calculations.[17] Similar to our previous work on aluminum surface,[18] four adsorbing sites were recognized on palladium <111> surface (figure 1). The nanoclusters applied here were Pd_{10}(7,3), Pd_7(4,3), Pd_7(6,1) and Pd_{10}(6,3,1), standing for on-top (O), bridge (B), and hollow (H1, H2) sites, respectively. In order to give bulk properties to these artificial nanoclusters and reduce the computational cost,[19] the distance of each two adjacent atoms (d) and layers(l) were fixed at the values of bulk,[20] i.e., 2.7506 and 2.2459 Å, respectively ($d = \frac{a}{\sqrt{2}}$, $l = \frac{a}{\sqrt{3}}$; a is the lattice constant).

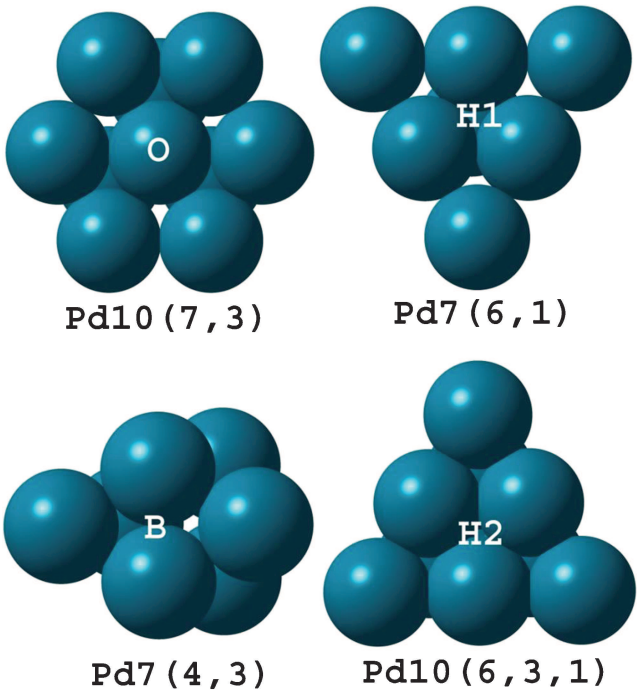

Figure 1. Four different adsorbing sites available on palladium <111> surface.

In the present density functional calculations, a relatively new high-level screened-hybrid-functional of Heyd-Scuseria-Enzerhof and Perdew-Burke-Ernzerhof, i.e., HSEh1PBE was applied (this functional is also referred to as HSE06 in the literature).[21–23] We applied HSEhPBE (HSE06), because it is able to produce good accuracy for solid, especially transition metals compounds, which typically are not well reproduced by conventional DFT functional,[24] at a reasonable computational cost. For geometry optimization, the palladium and hydrogen atoms were described using Stuttgart Dresden (SDD) and quadruple-zeta Dunning's correlation consistent (cc-pVQZ) localized basis sets, respectively.[25,26] In single point calculations, the basis sets were replaced by greater ones, i.e., by quadruple-zeta valance quality of Weigend and Ahlrichs (QZVP) and augmented cc-pV6Z, respectively.[27,28] Using these basis sets, we also determined the interaction of H atoms trapped in different interstices with tetrahedral (T_d) and octahedral (O_h) symmetries available in the palladium lattice (figure 2). Moreover, a cubic structure of interlocked T_d.Pd_4 and T_d.H_4 clusters was considered. By placing an additional H atom at the centre of the cube, a cubic-full nanocluster was also constructed. All present quantum chemical calculations were carried out at the lowest spin multiplicity[29–31] through *Gaussian 09* suite of computer codes[32] on a quad-core processor at 4 × 2.13 GHz clock speed.

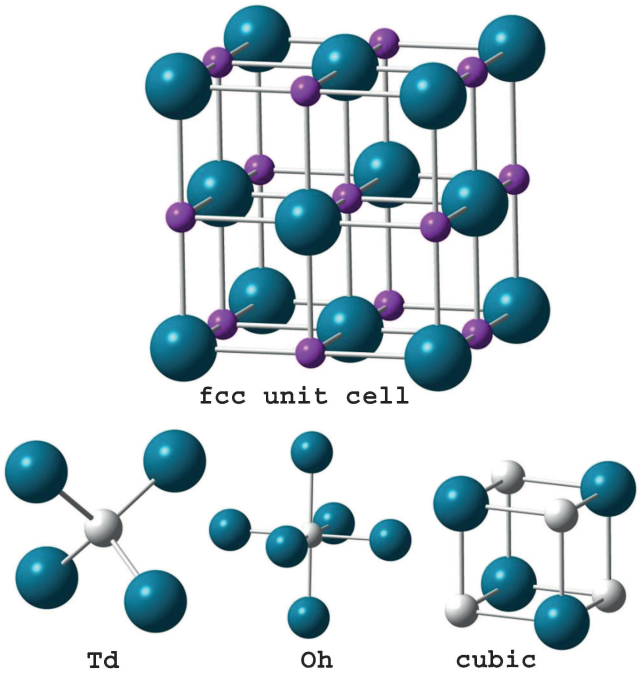

Figure 2. Schematic representation of the face centered cubic (fcc) palladium unit cell with its imaginable atomic voids (tetrahedral, Td and octahedral, Oh) occupied with hydrogen atoms (light spheres). The cubic is a hypothetical cell, consisting of two interlocked Td·Pd_4 and Td·H_4 nanoclusters.

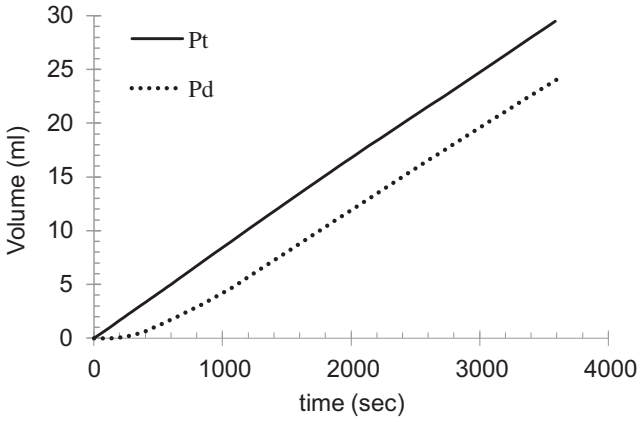

Figure 3. The volume of hydrogen gas evolving during water electrolysis process on palladium and platinum cathodes (surface area: 2.356 mm^2; current: 50 mA).

3. Results and Discussion

Figure 3 shows the volume of hydrogen gas evolved upon the Pd cathode. For comparison and better understanding the phenomenon (approval or disapproval of the results), we also carried out some complementary similar measurements upon another conventional electrode from the same group in the periodic table, i.e., platinum cathode (wire with the same dimension). From these gasometric investigations, the following results were deduced:

- By switching the electrolysis process on, the gas evolution starts immediately on Pt cathode but delayed by about 2 min on Pd one. After that, the gas evolution proceeds normally by appearing as tiny bubbles on the electrode surface.
- By cutting the electricity off, the gas evolution stops immediately on Pt wire whereas it lasts approximately one hour for Pd cathode.
- Under the same conditions, the volume of hydrogen gas that is evolved on Pt wire is greater than that on Pd wire.

The observations indicate three main processes: (1) proton reduction, (2) hydrogen adsorption (loading into palladium lattice) and (3) desorption (unloading process) as diatomic gas;

$$H^+ + e^- \rightleftarrows H_{ads} \quad (1)$$

$$H_{ads} \rightleftarrows H_{abs} \quad (2)$$

$$2H_{ads} \rightleftarrows H_2 \uparrow \quad (3)$$

Although Pd and Pt belong to the same group, the distinct behaviour of the electrodes seems to be the result of their different electronic configurations;[33] [Xe] $4f^{14}$ $5d^9$ $6s^1$ and [Kr] $4d^{10}$, standing for Pt and Pd atoms, respectively.

The electrochemical impedance spectra of palladium electrode were plotted in figure 4. The figure shows that the loading of hydrogen atoms into palladium lattice causes the diameter of semicircle being conspicuously decreased. The physical meaning of this observation is that the charge transfer resistance (R_{ct}) becomes correspondingly reduced.[3,15] Such behaviour was not observed for Pt electrode and the impedance of system remained unchanged (figure 5). However, the impedance of Pt electrode decreases significantly during the electrolysis process (figure 6). This is simply justifiable through the H atoms being transiently generated during the cathodic process (eq. 1) but not under open circuit condition (zero current).

The impedance spectra plotted in figures 4 and 6 can be divided into two parts: a depressed semicircle section followed by a horizontal/tangential tail at low frequencies. The first portion (depressed semicircle) is normally analyzed via a Randle-like equivalent circuit;[15] figure 7. Using this equivalent circuit, the values of R_{ct} along with other parameters were calculated and listed

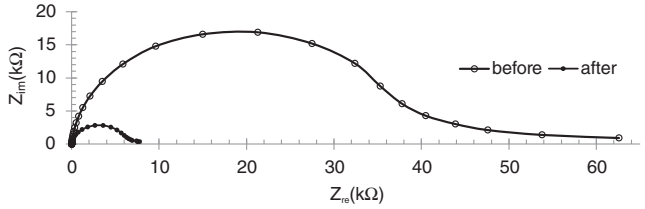

Figure 4. The influence of hydrogen absorption on impedance spectrum of Pd electrode, obtained at open circuit potential (OCP), before and after 30 min electrolysis; OCP's were -0.230 and $-0.808\ V_{SCE}$, respectively.

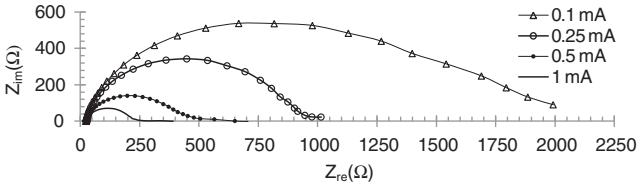

Figure 6. Impedance spectra of Pt electrode at different cathodic currents in 0.1 M NaOH solution.

in tables 1 and 2. The tables confirm the previous findings and indicate that the value of R_{ct} is noticeably decreased by loading the hydrogen atoms into the palladium lattice, or generating the transient H-atoms during the electrolysis process on the platinum cathode. Moreover, in the presence of H-loaded atoms, table 1 shows that the value of C_{PE} increases. This observation is justifiable through the charge creation phenomenon [notice the capacitance is defined as $C = q/V$], being atomistically witnessed through the Pd/H interactions (refer the next section). For the case of Pt, however, C_{PE} does not increase by increasing the cathodic current (table 2). This is also because of charge consumption/diminishing phenomenon being occurred at metal | solution interface, during the gas evolution process (see equations 1–3 and compare the values of C_{PE} under electrolysis and OCP conditions).

The latter portion of the impedance plots, i.e., the tangential/horizontal tail, is rather complicated to be modelled by a conventional/standard equivalent circuit. To interpret this interesting part of the diagram, one should notice that the tail appears at low frequencies, where enough time is available for hydrogen atoms to reach together, recombine and evolve as hydrogen gas. By desorption of hydrogen molecules, the number of charged particles decreases (refer equations 1–3) and hence the impedance of system will increase. Concerning the tangential line, it is worthy to note that at lower frequencies, the impedance of the constituting capacitor of the equivalent circuit approaches infinity $\left[|Z_c| = (2\pi\nu C)^{-1} \to \infty\right]$, so that the total equivalent circuit becomes simplified and acts as a pseudo-resistor; namely, its value depends on the hydrogen content in metal and varies with time (being gradually increased).

An atomic interpretation of the impedance decreasing due to the H-loading phenomenon, will be also presented in the next section (interactional studies), by means of charged particles, being created as the result of strong Pd/H interactions.

The potentio-dynamic response of both electrodes is illustrated in figures 8 and 9. The peaks in the extremes of these voltammograms (at potentials -1.2 and $1.1\ V_{SCE}$ for Pt; -1.45 and $1.15 V_{SCE}$ for Pd) correspond with the water electro-splitting reactions:

$$2H_2O + 2e^- \to H_2 \uparrow + 2OH^- \tag{4}$$

$$2H_2O \to 4H^+ + O_2 \uparrow + 4e^- \tag{5}$$

The middle peaks seeing in the voltammograms are related to the anodic oxidation of hydrogen atoms (H_{ads}; produced through eq. 1) and the cathodic reduction

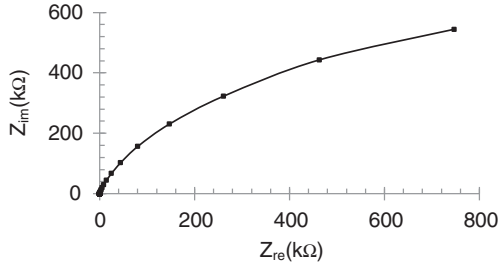

Figure 5. Impedance spectrum of Pt electrode obtained at OCP, $-0.068\ V_{SCE}$ (no difference was observed for the impedance of electrode before and after the electrolysis process).

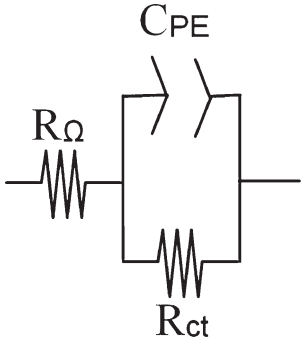

Figure 7. Randle-like equivalent circuit: R_Ω denotes ohmic or solution resistance, R_{ct} charge transfer resistance, and C_{PE} a double-layer pseudo-capacitance, so-called *constant phase element*.

Table 1. Electrochemical impedance parameters of palladium and platinum cathodes at OCP, determined before and after electrolysis processes, through Randle-like equivalent circuit.

Cathode	R_Ω (Ω cm^2)	R_{ct} (kΩ cm^2)	C_{PE} (μF/cm^2)
Pd (before)	5.4	8.9	16.1
Pd (after)	4.9	1.5	42.9
Pt (before/after)	3.3	36.6	192.7

($I < 0$) of oxygen molecules dissolved in the electrolyte. Both peaks disappear by deoxygenating the electrolyte solution and starting the potential scan from more positive values (above $-1.1\,V_{SCE}$, no hydrogen is produced and hence the corresponding peak disappears). Moreover, the peak intensity of hydrogen oxidation reaction observed for Pd is about five times greater than that of Pt electrode (figures 8 and 9). This is obviously because of H-sorption phenomenon witnessed formerly for Pd cathodes. By accepting this argument, we should also observe some peak enhancement/attenuation as the result of hydrogen loading (electrolysis)/unloading ($H_{ads} \rightarrow H^+ + e^-$) process. Figure 10 confirms this expectation. To determine the extent of hydrogen atoms diffused into palladium lattice, the atoms were oxidized at a constant anodic voltage.[34] By recording the current versus time (figure 11), the charge needing for oxidation/unloading process was computed ($Q = 25.8965$C, area under the curve). Figure 11 indicates that at the initial stages of the process, the current decreases sharply. In addition, most hydrogen atoms become oxidized during the first 3 h chronoamperometry. After 6 h, the current reaches $100\,\mu A$ and the process proceeds very slowly [the completion of the process takes about one day]. The other interesting result deducing from figure 11 is the transient halt detected at the initial stages of the unloading process. It is related to an isobar phase transition ($\beta \rightarrow \alpha$[35,36]) phenomenon taken place for PdH_x matrix, during the unloading process.[37] The halt recognized

Table 2. Electrochemical impedance parameters of platinum electrode during the electrolysis process, determined at different cathodic currents via Randle-like equivalent circuit.

Current (mA)	R_Ω (Ω cm^2)	R_{ct} (Ω cm^2)	C_{PE} (μF/cm^2)
0.10	6.1	330.8	53.1
0.25	6.2	196.0	51.4
0.50	6.1	86.9	48.4
1.00	6.0	42.5	47.5

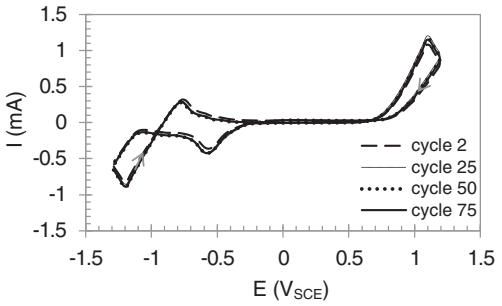

Figure 8. Cyclic voltammogram of Pt electrode in 0.1 M NaOH solution.

here is indeed similar to that witnessed elsewhere, by means of cooling-curve diagrams.[38]

The molar ratio of hydrogen to palladium atoms, x was calculated using this formula:

$$x = \frac{n_H}{n_{Pd}} = \frac{Q/F}{\rho_{Pd} \cdot V_{Pd}/M_{Pd}} = 9.1747 \times 10^{-5} Q/V_{Pd} \quad (6)$$

where V_{Pd} is the volume of electrode (in cm^3), Q the anodic charge (Coulomb), F faraday constant, ρ_{Pd} density, and M_{Pd} the atomic mass. The ratio obtained was 0.7883 ($PdH_{0.7883}$).

3.1 *Interactional studies*

The results of hydrogen interaction with different adsorbing sites on the palladium surface are given in table 3. The table indicates that the interactions are extremely high (1 Hartree=627.5095 kcal/mol) and interprets atomistically the inherent potency of palladium metal to attract the hydrogen atoms. Because of these strong forces, the hydrogen atoms are pulled closely and sank through the hollow or bridge voids (see figure 1 and notice the negative sign of d_H, presented in table 3). The tiny distance suggested by the

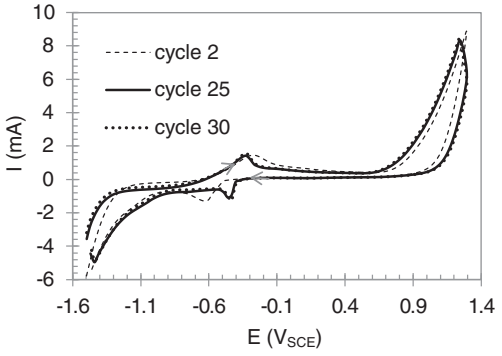

Figure 9. Cyclic voltammogram of Pd electrode in 0.1 M NaOH solution.

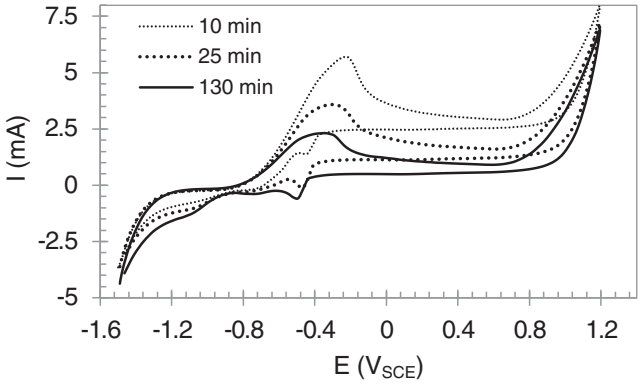

Figure 10. Cyclic voltammogram of Pd electrode (cycle 25) in 0.1 M NaOH solution after 30 min of electrolysis (50 mA), 4 hours rest, and oxidation of H_{ads}/H_{ads} (+200 mV_{SCE}) at different time intervals.

theory (0.27 Å) is also in accord with experiment.[39] Table 3 indicates that some negative (pseudo-hydride) species are produced by direct H interactions with palladium atoms (on-top sites), whereas the positive (proton-like) entities are created through the interactions with the remaining (bridge and hollow) sites. Because of the proton size (femtometer), they easily enter the interior of the metal lattice through the hollow and bridge voids. The driving force for this entrance (loading phenomenon; diffusion) is the gradient concentration (entropy increase) accompanied with the attractive forces exerted by the metal atoms in the bulk (table 4; the energies are comparable with those of hollows and bridge sites listed in table 3). The generation of charged particles also causes the impedance of the system being decreased as witnessed formerly via EIS measurements.

The charges listed in tables 3 and 4 were calculated through two different popular/standard procedures, i.e., Mülliken population and Merz-Singh-Kollman (MK) electrostatic analyses.[17,40,41] These charges are quite different from those formal oxidation states of hydrogen atom being conventionally reported in literature.[42] Although the values computed by these procedures are not similar, they both lead to the same trend with fair self-consistency ($R^2 \approx 0.97$).[7]

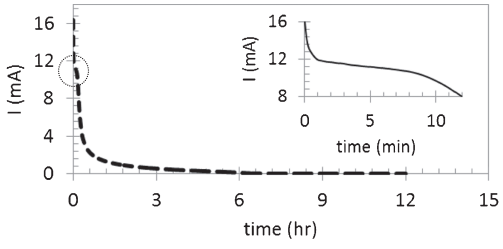

Figure 11. Chronoamperometry of Pd electrode in 0.1 M NaOH solution (+200 mV_{SCE}), after 30 min of electrolysis (50 mA) and 4 h rest.

Table 3. Hydrogen interaction (in atomic units) with different adsorbing sites upon the palladium surface (see also figure 1).

site	$E_{int.}$ [a]	d_H [b] (Å)	q_H [c]
O	−330.52220	0.27	(−0.18896, −0.10519)
B	−15.52350	−0.07	(0.84855, 0.34317)
H1	−8.29571	−0.13	(0.52627, 0.22420)
H2	−8.88984	−0.16	(0.48629, 0.12752)

[a]defined as $E_{int} = E_{Pd+H\,cluster} - (E_{Pd\,cluster} + E_H)$.[17]
[b]distance from surface; the negative sign means that the hydrogen atom is beneath the surface (penetrated the lattice).
[c]induced charge on hydrogen atom obtained by two popular methods, i.e., Mülliken population analysis and Merz-Singh-Kollman (MK) electrostatic procedure, respectively.[17]

Table 4. Some interactional data (in atomic units) of hydrogen atom(s) trapped in the palladium nanovoids (figure 2).

void symmetry	$E_{int.}$ [a]	d_{H-M}(Å)	q_H [b]
Td	−7.26498	1.68442	(0.27568, 0.38755)
Oh	−8.62550	1.94500	(0.23072, 0.47354)
Cubic	−14.68176	1.94500	(0.04953, −0.50286)
Cubic-full	−26.01310	1.94500	(0.13924, 0.39462)[c] (0.26803, −012713)[d]

[a]defined as $E_{int} = E_{Pd+H\,cluster} - (E_{Pd\,cluster} + E_{H\,cluster})$.[17]
[b]induced charge on hydrogen atom obtained from Mülliken population analysis and Merz-Singh-Kollman (MK) electrostatic procedures, respectively.[17]
[c,d]charges of hydrogen atoms occupied the center and the corner of the cubic cell, respectively.

Between octahedral (O_h) and tetrahedral (T_d) voids existing inside the palladium lattice, table 4 shows that the former interacts more strongly and the energy is comparable with that of H upon hollow sites. In addition, at the initial stages of the loading phenomenon, hydrogen atoms fill the lattice voids mostly in the cationic form and extra energy is released by occupying additional voids.

4. Conclusion

In the present study, we propose that hydrogen atoms enter the palladium lattice through the voids in the surface (hollows and bridge sites) as protons. The protons are generated by super-strong attractive forces and the generation of charged species (protons) causes

the impedance of system to be atomistically decreased during the H-loading phenomenon.

Acknowledgements

We gratefully acknowledge the anonymous Referee and the Editor for their constructive comments on this article.

References

1. Rigden J S 2003 In *Hydrogen: The essential element*, 3rd ed. (Massachusetts: Harvard University Press)
2. Nozik A J and Miller J R 2010 *Chem. Rev.* **110** 6443
3. Bockris J O'M, Reddy A K N and Gaboa-Aldeco M 2000 In *Modern electrochemistry* (New York: Kluwer Academic/Plenum Publishers) ch. **7** 13
4. Seife C 2004 *Science* **306** 1873
5. Fleischmann M, Pons S and Hawkins M 1989 *J. Electroanal. Chem.* **261** 301
6. Züttel A, Borgschulte A and Schlapbach L 2008 In *Hydrogen as a future energy carrier* (Weinheim: Wiley-VcH)
7. Lide D L 2003–2004 In *The CRC Handbook of Chemistry and Physics* 84th ed. (Oxford: CRC Press) pp. 4–22
8. Jewell L L and Davis B H 2006 *Appl. Catal. A: Gen.* **310** 1
9. Zeng K and Zhang D 2010 *Prog. Energy Combust. Sci.* **36** 307
10. Tavares S S M, Miraglia S, Fruchart D and Santos D S D 2002 *J. Alloys Compd.* **347** 105
11. Bard A J and Faulkner L R 2001 In *Electrochemical Methods: Fundamentals and Applications* (New York: John Wiley)
12. Vertova A, Rondinini S and Busca G 2002 *J. Appl. Electrochem.* **32** 661
13. Pacchioni G, Bagus P S and Parmigiani F 1992 In *Cluster Models for Surface and Bulk Phenomena* (New York: Plenum) pp. 267–359
14. Young D C 2001 In *Computational Chemistry: A Practical Guide for Applying Techniques to Real-World Problems* (New York: John Wiley) pp. 318–319
15. Barsoukov E and Macdonald J R 2005 In *Impedance Spectroscopy Theory, Experiment, and Applications* (New York: John Wiley)
16. Jaksic M M, Johansen B and Tunold R 1993 *Int. J. Hydrogen Energy* **18** 111
17. Lashgari M, Arshadi M R and Sastri V S 2007 *J. Electrochem. Soc.* **154** 93
18. Lashgari M and Malek A M 2010 *Electrochim. Acta* **55** 5253
19. Lashgari M, Arshadi M R and Biglar M 2010 *Chem. Eng. Comm.* **197** 1303
20. Avner S H 1974 In *Introduction to Physical Metallurgy* (New York: McGraw-Hill) p 86
21. Krukau A V, Vydrov O A, Izmaylov A F and Scuseria G E 2006 *J. Chem. Phys.* **125** 224106
22. Heyd J, Scuseria G E and Ernzerhof M 2006 *J. Chem. Phys.* **124** 219906
23. Paier J, Marsman M, Hummer K, Kresse G, Gerber I C and Ángyán J G 2006 *J. Chem. Phys.* **124** 154709
24. Chevrier V L, Ong S P, Armiento R, Chan M K Y and Ceder G 2010 *Phys. Rev. B* **82** 075122
25. Andrae D, Haeussermann U, Dolg M, Stoll H and Preuss H 1990 *Theor. Chem. Acc.* **77** 123
26. Woon D E and Dunning T H 1993 *J. Chem. Phys.* **98** 1358
27. Weigend F and Ahlrichs R 2005 *Phys. Chem. Chem. Phys.* **7** 3297
28. Wilson A K, Mourik T V and Dunning T H 1996 *J. Mol. Struct. (Theochem)* **388** 339
29. Nascimento M A C 2001 In *Theoretical Aspects of Heterogeneous Catalysis* (Dordrecht: Kluwer) p 230
30. Seminario J M and Tour J M 1997 *Int. J. Quantum Chem.* **65** 749
31. Bernardo C G P M and Gomes J A N F 2001 *J. Mol. Struct. (Theochem)* **542** 263
32. Frisch M J, Trucks G W, Schlegel H B, Scuseria G E, Robb M A, Cheeseman J R, Scalmani G, Barone V, Mennucci B, Petersson G A *et al.* 2009 *Gaussian 09* (Revision A.02, Inc., Wallingford CT)
33. Miessler G L and Tarr D A 2003 *Inorganic Chemistry*, 3rd ed. (New Jersey: Prentice-Hall) p 39
34. Vertova A, Rondinini S and Busca G 2002 *J. Appl. Electrochem.* **32** 661
35. Tripodi P, Armanet N, Asarisi V, Avveduto A, Marmigi A, Biberian J P and Vinko J D 2009 *Phys. Lett. A* **373** 4301
36. Lewis E A1994 *Platinum Met. Rev.* **38** 112
37. Łukaszewski M, Grdeń M and Czerwiński A 2004 *J. Electroanal. Chem.* **573** 87
38. Atkins P W and Paula J de 2006 *Physical chemistry*, 8th ed. (Oxford: Oxford Univ. Press) p 178
39. Gladys M J, Kambali I, Karolewski M A, Soon A, Stampfl C and O'Connor D J 2010 *J. Chem. Phys.* **132** 024714
40. Mülliken R S 1962 *J. Chem. Phys.* **36** 3428
41. Besler B H, Merz K M and Kollman P A 1990 *J. Comput. Chem.* **11** 431
42. Grochala W and Edwards P P 2004 *Chem. Rev.* **104** 1283